

Collisional Quenching of N_2O^+ A–X Emission by He, Ne, Ar, Kr, N_2 , CO, CO_2 , and N_2O

Takashi Imamura

Atmospheric Environment Division, The National Institute for Environmental Studies,
16-2 Onogawa, Tsukuba 305, Japan

Takashi Imajo

Department of Chemistry, Kyushu University, 33 Hakozaki, Higashiku, Fukuoka 812, Japan

Inosuke Koyano*

Department of Material Science, Himeji Institute of Technology, Kamigohri, Hyogo 678-12, Japan

Received: March 6, 1995; In Final Form: May 16, 1995*

Collisional quenching of N_2O^+ $\text{A}^2\Sigma^+[(0,0,0)$ and $(1,0,0)]$ by He, Ne, Ar, Kr, N_2 , CO, CO_2 , and N_2O has been investigated by a flowing afterglow technique combined with a time-resolved laser-induced fluorescence technique. The quenching rate constants by He and Ne are found to be 2 or 3 orders of magnitude smaller than the corresponding Langevin rate constant; the same situation as in the quenching of $\text{CO}^+(\text{A}, \nu=1)$. The quenching gases Ar, N_2 , CO, CO_2 , and N_2O , whose ionization potentials are lower than the recombination energy of $\text{N}_2\text{O}^+(\text{A})$, are found to deactivate $\text{N}_2\text{O}^+(\text{A})$ very efficiently, with a rate constant as large as the Langevin value. This fact would indicate the importance of the coupling between the $\text{N}_2\text{O}^+(\text{A})\text{--Q}$ and $\text{N}_2\text{O}\text{--}(\text{X})\text{--Q}^+$ states, where Q is a quenching gas. The rate constant for the quenching by Kr is much smaller than the Langevin value which can be ascribed to the unfavorable Franck–Condon factors between the $\text{N}_2\text{O}^+(\nu_1'=0, 1)\text{--Kr}$ states and the high vibrational states of $\text{N}_2\text{O X}(\nu'')\text{--Kr}^+$.

Introduction

Collisional deactivation processes of vibrationally and vibronically excited molecular ions are of particular interest in conjunction with their charge-transfer and chemical reactions. The $\text{A}^2\Pi$ state of CO^+ is one of the electronically excited states whose collisional quenching has been studied most extensively.^{1–11} In our previous work,^{8–10} it has been found that the mechanisms of the collisional quenching of $\text{CO}^+(\text{A}, \nu)$ can be divided into two groups depending on the nature of the quenching gas. That is, for the quenchers with a high ionization potential such as He and Ne, $\text{CO}^+(\text{A}, \nu)$ is deactivated slowly with a rate constant that is much smaller than the Langevin value. On the other hand, for quenchers with an ionization potential that is lower than the recombination energy of $\text{CO}^+(\text{A})$, such as Ar, the deactivation rate constant is as large as the Langevin value. The difference in the quenching efficiency is believed to be due to the availability of (a) charge transferred state(s) to interact with the reactant state.

For polyatomic molecular ions, no systematic study on the collisional deactivation of electronically excited states has been reported yet. N_2O^+ ion is known to emit in the near-ultraviolet region; $\text{A}^2\Sigma^+ \rightarrow \text{X}^2\Pi$.^{12–14} Fluorescence lifetimes of the $\text{A}^2\Sigma^+$ state of N_2O^+ have been measured under the collision-free conditions by several groups of authors using a variety of experimental techniques.^{15–18} From these investigations it seems to have been well established that the fluorescence lifetimes for the vibrationally excited states are shorter than that for the ground vibrational state. On the other hand, a photoelectron–photoion coincidence study has shown that the A $(0,0,0)$ state of N_2O^+ fluoresces to the $\text{X}^2\Pi$ state with a quantum yield of unity, whereas the fluorescence quantum yield from the $(1,0,0)$ level of the A state is reduced to 0.6.¹⁹ The shortening of the fluorescence lifetime and the decrease of the

fluorescence quantum yield by the vibrational excitation have been explained in terms of the predissociation of the A $(1,0,0)$ state into $\text{NO}^+ + \text{N}$ through the $^4\Sigma^-$ state. The only study of the collisional deactivation of $\text{N}_2\text{O}^+ \text{A}^2\Sigma^+$ reported so far is that of Ibuki and Sugita.²⁰ They found that both the $(0,0,0)$ and $(1,0,0)$ levels of the A state are quenched in collisions with the parent N_2O molecule with the quenching rate constant of $5 \times 10^{-10} \text{ cm}^3 \text{ molecule}^{-1} \text{ s}^{-1}$.²¹

Recently, Maier and co-workers have reported the electronic transitions in the $\text{N}_2\text{O}^+\text{--Ne}^{22}$ and $\text{N}_2\text{O}^+\text{--Ar}^{23}$ cluster systems by monitoring the fragment ions N_2O^+ and Ar^+ . They cannot find the NO^+ fragment ions in the excitation region of the A $\leftarrow \text{X}$ band in both systems, despite the importance of the predissociation through A $(\nu_1=1) \leftarrow \text{X}$ excitation for N_2O^+ monomer. Instead, they find strong charge-transfer bands in the 350–450 nm region in the $\text{N}_2\text{O}^+\text{--Ar}$ cluster system.

In the present paper, we measure the laser-induced fluorescence excitation spectra of $\text{N}_2\text{O}^+ \text{A} \leftarrow \text{X}$ and, using a time-resolved technique, study the collisional deactivation of the stable $(0,0,0)$ and predissociating $(1,0,0)$ levels of the $\text{A}^2\Sigma^+$ state by the collision with He, Ne, Ar, Kr, CO, N_2 , CO_2 , and N_2O . The quenching rate constants have been determined for all of them and the quenching mechanisms have been discussed.

Experimental Section

The experimental technique used is a conventional helium discharge flow technique combined with time-resolved laser-induced fluorescence detection, the details of which are described elsewhere.⁸ Briefly, N_2O^+ ions are prepared by Penning ionization with $\text{He}^*(^1^3\text{S})$, which is produced by a dc hollow-cathode discharge. N_2O^+ is excited to the $\text{A}^2\Sigma^+$ state in the observation region by a XeCl excimer laser pumped dye laser (Lambda Physik EMG 50/FL 3002). Fluorescence from the A state of N_2O^+ is collected and is focused on a slit of a

* Abstract published in *Advance ACS Abstracts*, October 1, 1995.

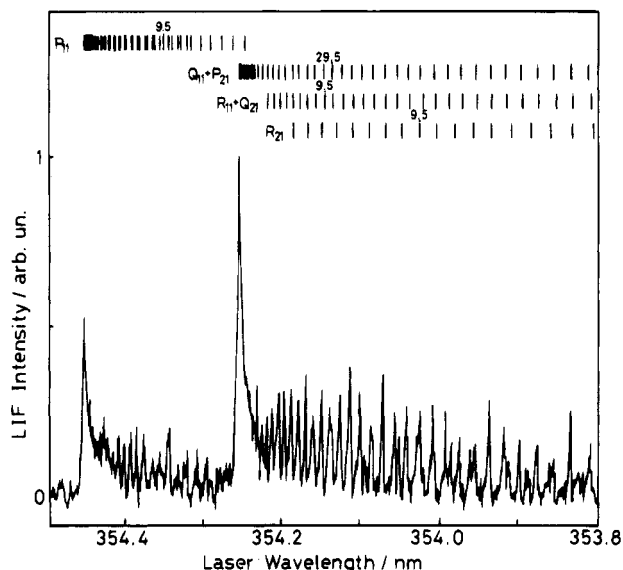


Figure 1. Laser-induced fluorescence excitation spectrum of the $A^2\Sigma^+(0,0,0) \leftarrow X^2\Pi_{3/2}(0,0,0)$ transition of N_2O^+ . Fluorescence was monitored at 387 nm.

monochromator (Nikon P-250) by a pair of lenses and is detected by a photomultiplier tube (Hamamatsu R928). The fluorescences from the $A(0,0,0)$ and $A(1,0,0)$ levels are monitored at 387 and 367 nm, respectively. Output signals are amplified by a wide-band preamplifier (NF BX-31) and are transferred to a digital oscilloscope (Lecroy 9450).

Research grade He or Ne is used as a carrier gas. Quenching gases, Ar, Kr, CO, N_2 , CO_2 , and N_2O , also of research grade, are introduced into the flow just upstream the detection area. Total pressure is monitored by a capacitance manometer (MKS Baratron). All experiments are carried out at room temperature (23 ± 3 °C).

Results

Figure 1 shows a laser-induced fluorescence excitation spectrum of N_2O^+ in the $A^2\Sigma^+(0,0,0) \leftarrow X^2\Pi_{3/2}(0,0,0)$ transition. Fluorescence was monitored at 387 nm ($A, v_1'=0 \rightarrow X, v_1''=2$ band). Rotational structure was partially resolved (wavelength resolution of the dye laser was 0.3 cm^{-1}). The assignment of the rotational lines shown in the figure is that appeared in the literature.¹² The rotational distribution in the $X^2\Pi$ state of our observed spectrum could be fitted by assuming the Boltzmann distribution at 295 K. This means that N_2O^+ does not dissociate so rapidly from high rotational levels of $A(0,0,0)$. The laser-induced fluorescence excitation spectrum of the $A(1,0,0) \leftarrow X^2\Pi_{3/2}(0,0,0)$ transition was also observed by monitoring fluorescence at 367 nm ($v_1'=1 \rightarrow v_1''=2$) and is shown in Figure 2. The $A(1,0,0)$ level has been known to be predissociating. From the excitation spectrum in Figure 2, no evidence is found for the rotationally selective predissociation.

Figure 3 shows the time profiles of the fluorescence intensity from the $(0,0,0)$ and $(1,0,0)$ levels of the $A^2\Sigma^+$ state, taken at the He pressure of 1.0 Torr. As shown in these figures, each profile could be fitted by a single-exponential decay function, from which the fluorescence lifetime was determined to be 249 ns for Figure 3a and 188 ns for Figure 3b. The fluorescence decay rates obtained for both vibronic levels were independent of the rotational level initially prepared. The shortening of the lifetime by the excitation of the v_1 vibration to $v_1=1$ in the $A^2\Sigma^+$ state has been explained in terms of the predissociation via the $a^4\Sigma^-$ state yielding $NO^+ + N$.

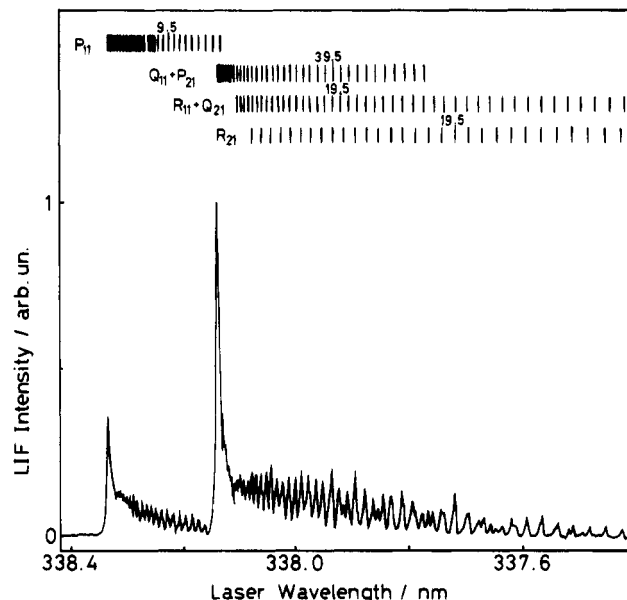


Figure 2. Laser-induced fluorescence excitation spectrum of the $A^2\Sigma^+(1,0,0) \leftarrow X^2\Pi_{3/2}(0,0,0)$ transition of N_2O^+ . Fluorescence was monitored at 367 nm.

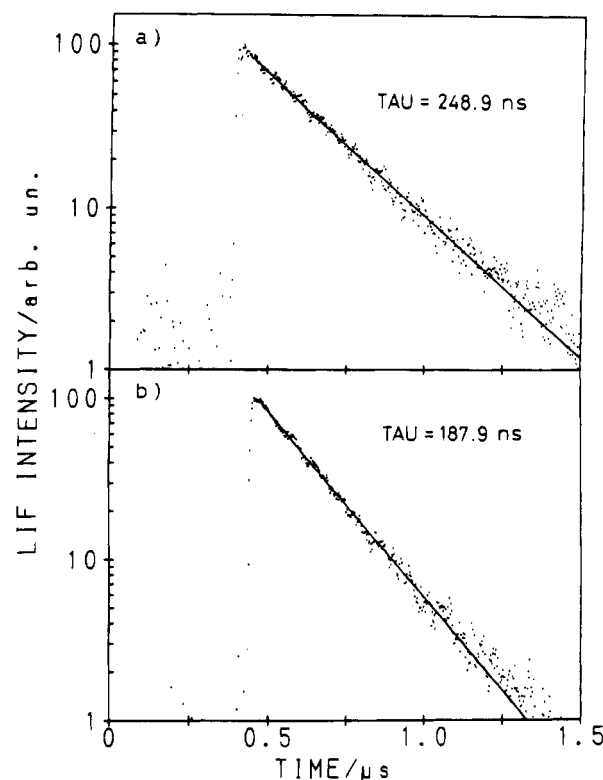


Figure 3. Time profiles of fluorescence intensity from the (a) $A^2\Sigma^+(0,0,0)$ and (b) $A^2\Sigma^+(1,0,0)$ levels. Total pressure and partial pressure of N_2O were 1.0 Torr and <3 mTorr, respectively.

An increase of the He pressure slightly decreased the fluorescence lifetime, τ_F , indicating that the carrier gas He somewhat quenches the $N_2O^+ A^2\Sigma^+$ in both vibrational levels. Figure 4 shows the Stern–Volmer plots ($k = 1/\tau_F$ vs He pressure) in the He/ N_2O system. The fluorescence decay rate, $k (= 1/\tau_F)$, is given by

$$k = 1/\tau_0 + k_{N_2O}[N_2O] + k_{He}[He]$$

where τ_0 represents the pressure independent lifetime of the $A^2\Sigma^+(0,0,0)$ level under our experimental conditions ($P_{He} = 1\text{--}5$

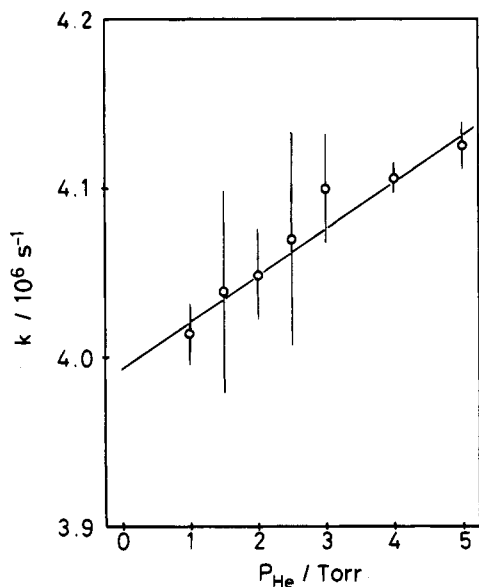


Figure 4. Fluorescence decay rates of N_2O^+ $\text{A}^2\Sigma^+(0,0,0)$ as a function of He pressure.

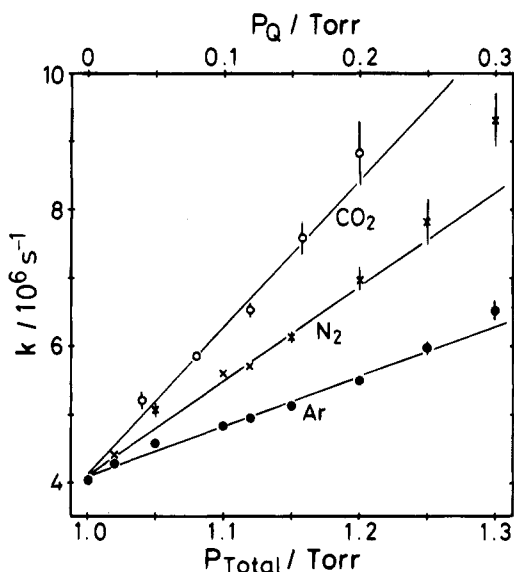


Figure 5. Fluorescence decay rates of N_2O^+ $\text{A}^2\Sigma^+(0,0,0)$ as a function of partial pressure of quenching gas Q (Q = Ar, N_2 , and CO_2).

Torr). $k_{\text{N}_2\text{O}}$ and k_{He} represent the collisional quenching rate constants by N_2O and He, respectively. From the slope of the fitted line in Figure 4, the k_{He} was determined to be $(8.5\text{--}4.8) \times 10^{-13} \text{ cm}^3 \text{ molecule}^{-1} \text{ s}^{-1}$. Neon has also been found to quench these vibronic states and quenching rate constants have been determined in a similar experiment using Ne in place of He as a carrier gas.

In studying the quenching by Ar, Kr, N_2 , CO_2 , N_2O , and CO, the quenching gas Q was introduced into the flow just upstream the detection area. Figure 5 shows the Stern-Volmer plots for the $\text{A}(0,0,0)$ level for Q = Ar, N_2 , and CO_2 . The fluorescence decay rate in this case is given by

$$k = 1/\tau_i + k_Q[\text{Q}]$$

where

$$1/\tau_i = 1/\tau_0 + k_{\text{N}_2\text{O}}[\text{N}_2\text{O}] + k_{\text{He}}[\text{He}]$$

The total removal rate constants, k_Q , by the collision with Ar, N_2 , and CO_2 were determined to be $(2.3 \pm 0.1) \times 10^{-10}$,

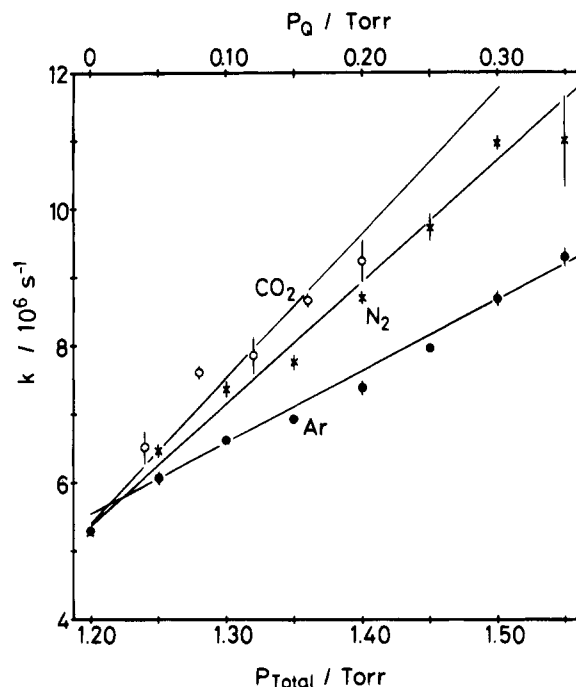


Figure 6. Fluorescence decay rates of N_2O^+ $\text{A}^2\Sigma^+(1,0,0)$ as a function of partial pressure of quenching gas Q (Q = Ar, N_2 , and CO_2).

$(4.3 \pm 0.2) \times 10^{-10}$, and $(6.7 \pm 0.3) \times 10^{-10}$, respectively, all in the unit of $\text{cm}^3 \text{ molecule}^{-1} \text{ s}^{-1}$.

The fluorescence lifetimes measured in the $\text{He}/\text{N}_2\text{O}/\text{Q}$ systems were also found to be independent of the rotational level initially prepared. Moreover, the fluorescence excitation spectrum of the $\text{A}(0,0,0) \leftarrow \text{X}(0,0,0)$ band measured in the $\text{He}/\text{N}_2\text{O}/\text{N}_2$ (the partial pressure of $\text{N}_2 = 0.2$ Torr) system showed no apparent change from the spectrum observed in the $\text{He}/\text{N}_2\text{O}$ system. These facts suggest that the total removal rate constants obtained are characteristic of the vibrational state and not of particular rotational state.

The Stern-Volmer plot for the quenching of the $\text{A}(1,0,0)$ level by Ar, N_2 , and CO_2 are shown in Figure 6. The decay rates were again insensitive to the rotational levels initially prepared. The total removal rate constants obtained from the slopes of the plots are $(3.2 \pm 0.2) \times 10^{-10}$ for Ar, $(5.5 \pm 0.3) \times 10^{-10}$ for N_2 , and $(6.5 \pm 0.4) \times 10^{-10}$ for CO_2 all in the unit of $\text{cm}^3 \text{ molecule}^{-1} \text{ s}^{-1}$. The total removal rate constants for the $(0,0,0)$ and $(1,0,0)$ levels of the $\text{A}^2\Sigma^+$ state by several quenchers studied in the present work are listed in Table 1 together with the Langevin rate constants.

Discussion

The partial pressure of N_2O added as a precursor of N_2O^+ was lower than 3 mTorr in all experiments. The quenching rate of N_2O^+ $\text{A}^2\Sigma^+$ by precursor N_2O itself is then estimated to be $< 5 \times 10^4 \text{ s}^{-1}$ on the basis of the total removal rate constant obtained here. The intercept with the y axis of the Stern-Volmer plot for N_2O^+ $\text{A}(0,0,0)$ in the $\text{He}/\text{N}_2\text{O}$ system is $4 \times 10^6 \text{ s}^{-1}$ as shown in Figure 4. This implies that the quenching by the trace of N_2O existing in the system hardly affects the decay rates of the $\text{A}(0,0,0)$ level of N_2O^+ by added quenchers Q. The zero-pressure lifetime, τ_0 , was determined to be 250 ± 3 ns for the $\text{A}(0,0,0)$ level. According to the photoelectron-photoion coincidence study of Eland,¹⁹ the fluorescence quantum yield of the $\text{A}(0,0,0)$ level is unity under the collision free conditions. This indicates that τ_0 is identical to the radiative lifetime, τ_r . The τ_r value of the $\text{A}(0,0,0)$ level obtained here is in good agreement with those reported previously.^{15-18,20}

TABLE 1: Collisional Quenching Rate Constants (in 10^{-10} cm³ molecule⁻¹ s⁻¹) for the A²Σ⁺ State of N₂O⁺

	(0,0,0)	(1,0,0)	K_L^a
He	$(8.5 \pm 4.8) \times 10^{-3}$	$(7.5 \pm 5.2) \times 10^{-3}$	5.5
Ne	$< 10^{-2}$	$(4.8 \pm 1.2) \times 10^{-2}$	4.0
Ar	2.3 ± 0.1	3.2 ± 0.2	6.6
Kr	$(7.7 \pm 7.6) \times 10^{-2}$	$< 10^{-2}$	6.9
N ₂	4.3 ± 0.2	5.5 ± 0.3	7.5
CO ₂	6.7 ± 0.3	6.5 ± 0.4	8.1
N ₂ O	3.8 ± 0.7	4.7 ± 0.5	8.6
	$[5.2 \pm 0.2]^c$	$[5.0 \pm 0.3]^c$	
CO	$[\sim 4]^d$		7.9
	1.5 ± 0.7		
	$[\sim 3]^d$		
	$[5.7]^e$		

^a Langevin rate constant = $2\pi e\sqrt{\alpha/\mu}$ where α is the average polarizability of the quencher, and μ the reduced mass. ^b Errors quoted are 2σ of the standard deviation. ^c Collisional quenching rate constants reported by Ibuki and Sugita.²¹ ^d Reaction rate constant of N₂O⁺(X²Π) reported by Kemper and Bowers.²⁵ ^e Reaction rate constant of N₂O⁺(X²Π) reported by Jones et al.²⁶

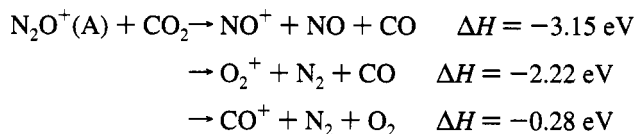
Similarly, the τ_0 value of the A(1,0,0) level was determined to be 192 ± 3 ns. The A(1,0,0) level has been known to be predissociating.^{15–20} Assuming that the radiative lifetime of the (1,0,0) level is identical to that of the (0,0,0) level, the predissociation rate is estimated to be 1.2×10^6 s⁻¹. The value again is in good agreement with those reported in the literature.^{15–18,20}

The total removal rate constants in collisions with He and Ne are of the order of 10^{-12} – 10^{-13} cm³ molecule⁻¹ s⁻¹. The ionization potentials (IPs) of both quenchers, 24.6 and 21.6 eV for He and Ne, respectively, are much larger than the recombination energy (RE) of the A state of N₂O⁺, 16.4 eV. Thus, no charge transfer (CT) interactions are expected during collisions with these quenchers. On the other hand, the possibility that these nontrivial quenching rate constants are due to impurities in the He and Ne samples is ruled out because the expected contents of impurities are much smaller than 100 ppm (purity claimed by the supplier is 99.9999%). Thus there must be some mechanism(s), other than the charge transfer, that deactivate(s) A(0,0,0) and A(1,0,0) states of N₂O⁺ slowly. For the A²Π state of CO⁺, previous studies have shown that the quenching by He and Ne induces the internal conversion to the X²Σ state¹⁰ and its rate constant is dependent on the Franck–Condon factors (FCFs) between the A²Π(ν) and the adjacent X(ν') levels.² In the case of N₂O⁺, the geometrical change in going from the X to A states is not so large and therefore the FCFs between the A($\nu_1, 0, 0$) ($\nu_1 = 0$ or 1) and the adjacent high vibrational levels (including ν_1 , ν_2 , and ν_3 modes) of the X state would be significantly smaller than that between, for example, the A($\nu=1$) and adjacent X($\nu=11$) levels of CO⁺. Nevertheless, the quenching rate constants of N₂O⁺(A) by He and Ne obtained in the present work are of the same order of magnitude as those of CO⁺(A). The reason for this is not clear at present, however. The quenching by He and Ne would perhaps be due to the mixing between the Π and Σ states.

Contrary to He and Ne, the IP's of Ar (15.8 eV) and Kr (14.0 eV) are smaller than the RE of N₂O⁺ A²Σ⁺, and thus the CT interaction is considered to be the dominant quenching mechanism for these quenchers. Since the CT states are energetically accessible for these quenchers, both Ar and Kr are expected to quench N₂O⁺(A) efficiently. However, the quenching rate constant by Kr was found to be much smaller than that of Ar despite the fact that their Langevin rate constants are not largely different from each other. A large difference existing between the N₂O⁺(A, $\nu_1=0$) + Ar and N₂O⁺(A, $\nu_1=0$) + Kr systems is

that in the energy gap between the reactant and product states: the energy gaps are 0.5 and 2.4 eV for N₂O⁺(0,0,0)–Ar⁺(²P_{3/2}) and N₂O–Kr⁺, respectively. The FCFs between N₂O⁺(A, ν') and N₂O(X, ν'') states are expected to have large values only in the case of $\nu'' \sim \nu'$ owing to their structural similarity. Indeed, the FCFs for the N₂O⁺ A²Σ⁺($\nu_1, 0, 0$) ← N₂O X¹Σ⁺(0,0,0) transitions have been reported to be 0.749 for $\nu_1=0$ and 0.164 for $\nu_1=1$ from photoelectron spectroscopy.²⁴ The large energy gap thus leads to unfavorable FCFs, which is thought to be responsible for the inefficient collisional deactivation by Kr. For the quenching by Ar, we could not find any significant difference in the quenching rate constants between the stable (0,0,0) and predissociating (1,0,0) levels. In the photofragmentation study of the N₂O⁺–Ar cluster,²³ it was reported that both N₂O⁺ and Ar⁺ ions were formed by the photoexcitation in the region of the A ← X transition of N₂O⁺ monomer but no NO⁺ fragment ions could be detected. This result strongly lends support to our interpretation that, the efficient quenching by Ar is due to the CT reaction.

N₂ and CO₂ are diatomic and triatomic molecules with no permanent dipole. The IP's of N₂ and CO₂ are 15.6 and 13.8 eV, respectively, both of which are smaller than the RE of N₂O⁺–(A). These molecules were found to quench the N₂O⁺ fluorescence efficiently with a rate constant of the same order of magnitude as the corresponding Langevin's one. Especially, it is noteworthy that the rate constant of CO₂ is much larger than that of Kr despite the fact that their IPs are similar. The reason for this is not clear, but may be in the difference in the nature of the interaction and/or the degrees of freedom that can accept disposed energy. In addition, several chemical channels such as



are energetically possible with CO₂. Unfortunately, however, we cannot be certain, without a mass spectrometer, which possibilities are actually responsible for the above difference between the Kr and CO₂ quenchers. No significant difference was found in the quenching rate constants of N₂ and CO₂ between the stable (0,0,0) and predissociating (1,0,0) levels. From the present study, it is difficult to make the mechanisms of collisional quenching by N₂ and CO₂ clear, but here again the interaction between the N₂O⁺(A)–Q and N₂O–Q⁺ states might play an important role for the quenching.

N₂O is known to react with N₂O⁺(X) with the rate constant of 4×10^{-10} cm³ molecule⁻¹ s⁻¹.²⁵ As a reaction channel, CT reaction has been reported to be dominant (98%). Furthermore, the reaction of N₂O⁺ + N₂O was thought to proceed by direct charge transfer without forming an intermediate complex.²⁵ In the present study, N₂O was found to quench N₂O⁺(A) as efficiently as its reaction with N₂O⁺(X). The quenching rate constants for the A(0,0,0) and A(1,0,0) states were determined to be $(3.8 \pm 0.7) \times 10^{-10}$ and $(4.7 \pm 0.5) \times 10^{-10}$ cm³ molecule⁻¹ s⁻¹, respectively. These value are slightly smaller than those reported by Ibuki and Sugita,²¹ but the reason for this discrepancy is not clear at this stage. Although the quenching rate constants are comparable to the rate constant of the N₂O⁺(X) + N₂O reaction, whose mechanism is thought to be a direct charge transfer, the CT reaction of N₂O⁺(A) + N₂O(X) → N₂O(X) + N₂O⁺(X, ν) seems to be inefficient due to poor FCFs for high ν 's. So, the fast quenching of N₂O⁺(A) by N₂O might be due to some chemical reactions.

CO is also found to quench $\text{N}_2\text{O}^+(\text{A})$ efficiently, with the rate constant of $(1.5 \pm 0.7) \times 10^{-10} \text{ cm}^3 \text{ molecule}^{-1} \text{ s}^{-1}$ (Table 1). The reactions of CO with the ground-state $\text{N}_2\text{O}^+(\text{X})$ ions have previously been studied by Jones et al.²⁶ using a SIFT technique and by Kemper and Bowers²⁵ using an ICR technique. Both groups report the dominant ($\sim 100\%$) product channels to be $\text{NO}^+ + \text{NCO}$ and $\text{CO}_2^+ + \text{N}_2$, but with somewhat different branching ratios. The overall reaction rate constants reported by the two groups are 5.7×10^{-10} and $3.0 \times 10^{-10} \text{ cm}^3 \text{ molecule}^{-1} \text{ s}^{-1}$, respectively (the latter authors noted that the rate constant depends on KE between 0.1 and 4 eV). The latter authors also proposed both reactions proceed via formation of a linear intermediate complex. In our present study with excited $\text{N}_2\text{O}^+(\text{A})$, we do not know the product channels of the deactivation, unfortunately. However, it is unlikely that the products are also $\text{NO}^+ + \text{NCO}$ or $\text{CO}_2^+ + \text{N}_2$, since $\text{N}_2\text{O}^+(\text{A}^2\Sigma^+) + \text{CO}(^1\Sigma)$ does not directly correlate to $\text{NO}^+(^1\Sigma) + \text{NCO}(^2\Pi)$ nor to $\text{CO}_2^+(^2\Pi) + \text{N}_2(^1\Sigma)$ owing to the nonconservation of angular momentum in the linear configuration. Thus the large quenching rate constant obtained here suggests the occurrence of some new mechanism available to the excited $\text{A}^2\Sigma^+$ state. Here again, we note that the CT process forming $\text{CO}^+ + \text{N}_2\text{O}$, which is an endothermic channel for the $\text{N}_2\text{O}^+(\text{X}) + \text{CO}$ system, is energetically possible for the $\text{N}_2\text{O}^+(\text{A}) + \text{CO}$ system. These facts perhaps indicate that the quenching of $\text{N}_2\text{O}^+(\text{A})$ by CO proceeds via the coupling between the $\text{N}_2\text{O}^+(\text{A})$ –CO and $\text{N}_2\text{O}(\text{X})$ – $\text{CO}^+(\text{X})$ states rather than the formation of linear complexes proposed for the $\text{N}_2\text{O}^+(\text{X}) + \text{CO}$ system. The importance of such CT interaction during collisions in deactivation of electronically or vibronically excited ions has also been demonstrated in our previous studies of collisional quenching of $\text{CO}^+ \text{A}^2\Pi(v = 0-2)$ with various atoms and molecules.⁸⁻¹⁰

Conclusions

A flowing afterglow/time-resolved laser-induced fluorescence technique has been used to investigate the deactivation processes of vibronically excited triatomic molecular ions, $\text{N}_2\text{O}^+ \text{A}^2\Sigma^+$ –(0,0,0) and (1,0,0), in collisions with a series of atoms and molecules. Room temperature rate constants have been determined for quenching molecules He, Ne, Ar, Kr, N_2 , CO, CO_2 , and N_2O . The rate constants for quenchers He, Ne, and Kr, have been found to be 2 or 3 orders of magnitude smaller than the corresponding Langevin rate constant, while those for other quenchers have values as great as the corresponding Langevin rate constant. Furthermore, the quenchers of the former group generally (except He) exhibit different magnitudes of the rate constant for the two vibrational states (0,0,0) and (1,0,0), whereas the quenchers of the latter group show more or less the same magnitude of rate constant for the two vibrational states. This trend is in line with the results of our previous studies of collisional deactivation of $\text{CO}^+ \text{A}^2\Pi(v=0-2)$.

The difference in the quenching behavior between the two groups of quenchers have been interpreted in terms of the availability of (a) energetically accessible CT state(s) with the latter group of quenchers. It has been stressed that the charge-transfer interaction during collisions is important in order for as efficient deactivation to occur. Kr is exceptional in this

context, since its IP is smaller than the recombination energy of $\text{N}_2\text{O}^+(\text{A})$ and yet shows very small quenching rate constants. Its exceptionally low deactivation efficiency has been ascribed to the unfavorable FCFs between the $\text{N}_2\text{O}^+(\text{A})(0,0,0)/(1,0,0)$ states and the higher vibrational states including all vibrational mode of neutral N_2O . Such high vibrational states of neutral N_2O must certainly be involved in the quenching process owing to the large energy gap between the $\text{N}_2\text{O}^+(\text{A}) + \text{Kr}$ and $\text{N}_2\text{O} + \text{Kr}^+$ states.

To confirm the interpretation proposed here, it would be necessary to detect the final CT products mass spectrometrically in a state-selected study, as has been done with the $\text{CO}^+(\text{A}^2\Pi, v) + \text{Ar}$ system¹⁰ using our TESICO technique.²⁷ However, such measurements are extremely difficult for the present reaction systems because of the short lifetime of the $\text{N}_2\text{O}^+(\text{A})$ state, even with the single-chamber mode of the TESICO operation.

Acknowledgment. This work was partially supported by Grants-in-Aid for Scientific Research Nos. 03403003 and 06209208 from the Japanese Ministry of Education, Science, and Culture.

References and Notes

- (1) Bondybey, V. E.; Miller, T. A. *J. Chem. Phys.* **1978**, *69*, 3597.
- (2) Katayama, D. H.; Welsh, J. A. *J. Chem. Phys.* **1983**, *79*, 3627.
- (3) Katayama, D. H.; Welsh, J. A. *Chem. Phys. Lett.* **1984**, *106*, 74.
- (4) Dentamaro, A. V.; Katayama, D. H. *J. Chem. Phys.* **1994**, *101*, 8628.
- (5) Ibuki, T.; Sugita, N. *J. Chem. Phys.* **1983**, *79*, 5392.
- (6) Danon, J.; Mauclaire, G.; Govers, T. R.; Marx, R. *J. Chem. Phys.* **1982**, *76*, 1255.
- (7) Lemaire, J.; Marx, R.; Parent, D. C.; Chevrier, M. *J. Chem. Phys.* **1990**, *92*, 1653.
- (8) Imajo, T.; Imamura, T.; Koyano, I. *Chem. Phys. Lett.* **1989**, *160*, 143.
- (9) Imamura, T.; Imajo, T.; Koyano, I. *Chem. Phys. Lett.* **1991**, *178*, 399.
- (10) Imamura, T.; Imajo, T.; Suzuki, S.; Koyano, I. *J. Chem. Phys.* **1993**, *98*, 6348.
- (11) Imajo, T.; Imamura, T.; Koyano, I. *Chem. Phys. Lett.* **1994**, *223*, 99.
- (12) Callomon, J. H.; Creutzberg, F. *Philos. Trans. R. Soc. London* **1974**, *30*, 175.
- (13) Tsuji, M.; Tsuji, K.; Nishimura, Y. *Int. J. Mass Spectrom. Ion Phys.* **1979**, *30*, 175.
- (14) Tsuji, M.; Maier, J. P. *Chem. Phys.* **1988**, *126*, 435.
- (15) Frey, R.; Gotchev, B.; Peatman, W. B.; Pollak, H.; Schlag, E. W. *Chem. Phys. Lett.* **1978**, *54*, 411.
- (16) Maier, J. P.; Thommen, F. *Chem. Phys.* **1980**, *51*, 319.
- (17) Klapstein, D.; Maier, J. P. *Chem. Phys. Lett.* **1981**, *83*, 590.
- (18) Smith, W. H. *J. Chem. Phys.* **1969**, *51*, 3410.
- (19) Eland, J. H. D. *Int. J. Mass Spectrom. Ion Phys.* **1973**, *12*, 389.
- (20) Ibuki, T.; Sugita, N. *J. Chem. Phys.* **1984**, *80*, 4625.
- (21) Ibuki, T., private communication. The quenching rate constants of the A state of N_2O^+ reported by Ibuki and Sugita (Table 1 in ref 20) should be read as $(5.21 \pm 0.16) \times 10^{-10}$ for $v_1 = 0$ and $(5.04 \pm 0.26) \times 10^{-10}$ for $v_1 = 1$ all in the unit of $\text{cm}^3 \text{ molecule}^{-1} \text{ s}^{-1}$.
- (22) Soliva, A. M.; Bieske, E. J.; Maier, J. P. *Chem. Phys. Lett.* **1991**, *179*, 247.
- (23) Bieske, E. J.; Soliva, A. M.; Friedmann, A.; Maier, J. P. *J. Chem. Phys.* **1992**, *96*, 7535.
- (24) Brundle, C. R.; Turner, D. W. *Int. J. Mass Spectrom. Ion Phys.* **1969**, *2*, 195.
- (25) Kemper, P. R.; Bowers, M. T. *Int. J. Chem. Kinet.* **1984**, *16*, 707.
- (26) Jones, J. D. C.; Birkinshaw, K.; Twiddy, N. D. *J. Phys. B: At. Mol. Phys.* **1981**, *14*, 2705.
- (27) Koyano, I.; Tanaka, K. *J. Chem. Phys.* **1980**, *72*, 4858.

JP950631T